Synthesis of the driving functions of an array for propagating localized wave energy

J. E. Hernandez, R. W. Ziolkowski,[a] and S. R. Parker[b]
Lawrence Livermore National Laboratory, University of California, P.O. Box 808 L-156, Livermore, California 94450

(Received 7 November 1990; revised 11 February 1992; accepted 26 February 1992)

This paper presents a framework for designing the driving functions of an array of radiating elements given a scalar representation of the desired propagating field at a finite number of remote spatial locations. Based on a point source propagation model in a homogeneous media, the relationship between the driving functions and the resulting field leads to a system of linear equations in the frequency domain. A least-squares solution to the inverse problem is obtained by solving the system of linear equations for the unknown array driving functions. The proposed framework is suitable for designing array driving functions that could be used to generate "source-free" (homogeneous) solutions to the wave equation. This paper focuses on the use of the proposed technique for calculating array driving functions for generating localized wave energy. Two cases are discussed; one based on a source-free solution to the wave equation, and the other based on a numerical traveling impulse function. The results are compared to the beam generated by driving the array uniformly with a continuous-wave (cw) signal.

PACS numbers: 43.20.Rz, 43.30.Vh, 43.30.Wi, 43.30.Yj

LIST OF SYMBOLS

t	discrete time variable
(x,y,z)	Cartesian coordinates
$f(t,x,y,z)$	function of the variables t,x,y,z
$f_i(t)$	the i th function
$F(\omega)$	Fourier transform: $F(\omega) = \int f(t) e^{-(\omega t\sqrt{-1})}\, dt$
π	pi = 3.1416
τ	fixed time
ω	angular frequency
c	velocity of propagation
$\sum^{i}$	sum for all i
$\sum^{t}$	sum over all discrete times values
j	square root of -1
$*$	complex conjugate
$\frac{\partial}{\partial x} f(\ )$	partial derivative of $f(\ )$ with respect to x
$\partial_t g(\ )$	partial derivative of $g(\ )$ with respect to t
$\mathbf{f}$	column vector
$\|\mathbf{f}\|_2$	squared (L_2) norm of a vector
$\mathbf{H}$	matrix
$\mathbf{H}^{\dagger}$	complex-conjugate transpose of $\mathbf{H}$
$\mathbf{H}^{-1}$	inverse of $\mathbf{H}$
$\mathbf{I}$	identity matrix
$\int^{t} f(\ )dt$	integral of $f(\ )$ from $-\infty$ to t
$\int f(\ )dt$	integral of $f(\ )$ from $-\infty$ to $+\infty$

INTRODUCTION

New solutions to the wave equations have been recently discovered which support the possibility of transmitting localized, slowly decaying pulses of finite energy known as localized waves (LW).[1] Because the LW are "source-free" solutions to the wave equation, much time has been devoted to finding a launching mechanism capable of generating these special solutions. Ziolkowski[1] has proposed the use of independently addressable, pulse driven antennas as the physical launching mechanism. The basic idea is to drive a finite array of radiating elements (each element can be excited independently from the other) to produce the desired LW field. It is desired that given enough elements in an array of a specified size, the transmitted field energy remains localized for a reasonable range of distances.

It has been verified through computer simulations that it is possible to generate LW solutions to the wave equation over a limited range of distances using a finite-sized array of radiating elements.[1] This is achieved by driving a finite planar array of point sources with the appropriately shaped pulses. The driving function for each array element is a broad-bandwidth waveshape determined by the exact LW solution and its derivatives. These functions correspond to those required by a Huygens representation of the array generated wave field. Although in theory the array should be infinite and continuous to recover the exact field at every space-time point, the results show that it is possible to obtain

[a] Associate Professor, Department of Electrical and Computer Engineering, The University of Arizona.
[b] Consultant at LLNL, E. E. Dept., Information Systems Lab., Stanford University.

 0001-4966/92/070550-13$00.80

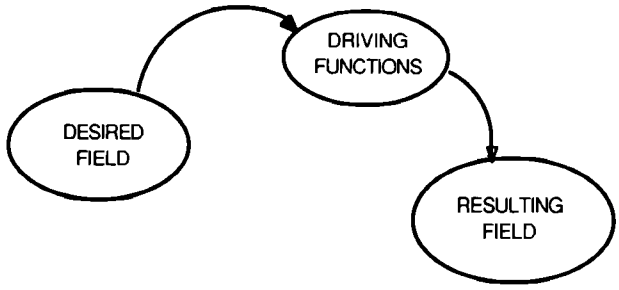

FIG. 1. The desired field is used to calculate a set of optimum driving functions to produce a field similar to the desired field.

reasonably localized beam fields with a finite-sized array.

We are currently investigating ways to reduce the aperture size of the array as well as the number of array elements and still be able to generate the LW solution. One approach consists of finding ways to squeeze a large array into a smaller one by driving the array with a more complicated set of pulse shapes whose functions are derived from the original solutions within the array aperture and beyond it.[1] The solutions beyond the maximum distance are "folded" into the interior of the array in a particular way, trading a simple source distribution for a more complicated one.

Another approach is to use optimization techniques to find driving functions that will "best" match: (1) LW solutions or (2) an ideal "traveling-impulse." The approach is illustrated in Fig. 1. Basically, the desired field is specified at a finite number of spatial locations. Field samples are then used to calculate an optimum set of driving functions that will produce a field similar to the desired field.

In Sec. I, we formulate the least-squares solution to the LW inverse propagation problem. Based on a point source propagation model in a homogeneous media, a relationship between the driving functions and the desired field is formulated which leads to a set of linear equations in the frequency domain. The least-squares solution to the inverse problem is then obtained by solving the system of linear equations for the unknown array driving functions. In Sec. III, we demonstrate the use of the proposed technique for calculating array driving functions for generating localized wave energy. Two different cases are investigated. In the first case, an LW solution to the wave equation is used as the desired field. The resulting field is compared to the field generated from a Huygens reconstruction which has been the traditional way of calculating array driving functions to generate source-free solutions to the wave equation. A discussion on how to sample the desired field is included. In the second case, a numerical traveling impulse function is specified as the desired field. All the results are then compared to the traditional continuous wave (cw) or monochromatic case. The last section discusses the results and suggests some areas of future work. Several possible alternate approaches to solving the inverse problem are discussed in the Appendix.

I. PROBLEM FORMULATION

In this section, we formulate a mathematical model for designing the driving functions of an array of point sources given the desired field at a finite number of spatial locations. We will be considering acoustic pulses that satisfy the scalar wave equation in a homogeneous media with a constant speed of propagation.

A. Field generated by an array of point source

The field generated at some arbitrary location in space due to a single point source is given by

$$g(t,x,y,z) = f(t-\tau,x_0,y_0,z_0)/(4\pi r), \tag{1}$$

where $f(\ )$ is the driving function, $g(\ )$ is the resulting field, τ is the propagation delay, r is the traveled distance, and x_0,y_0,z_0 are the spatial coordinates of the point source. Based on the principle of superposition, the field generated at some arbitrary location in space due to an array of point sources is then given by

$$g(t,x,y,z) = \sum^{i} \frac{f_i(t-\tau_i,x_i,y_i,z_i)}{(4\pi r_i)}, \tag{2}$$

where i is the array element index, τ_i is the propagation delay from the i th array element, r_i is the traveled distance from the i th array element, and x_i,y_i,z_i are the spatial coordinates of the i th array element. In general, the field generated at some arbitrary set of locations in space due to an array of point sources is given by

$$g_j(t) = \sum^{i} \frac{f_i(t-\tau_{ij})}{(4\pi r_{ij})}, \quad 1 \leqslant i \leqslant L, \quad 1 \leqslant j \leqslant M, \tag{3a}$$

where i is the array element index, j is the field spatial location index, τ_{ij} is the propagation delay from the i th element to the j th location, r_{ij} is the traveled distance from the i th element to the j th location, L is the total number of array elements, and M is the total number of field locations. Note that in order to simplify the notation, we have omitted the dependency of the functions $f(\ )$ and $g(\ )$ on the spatial coordinates (x,y,z) in Eq. (3a). Nevertheless, the spatial coordinates (x,y,z) of the array as well as the field locations are needed in order to calculate the propagation delays (τ_{ij}) and the traveled distances (r_{ij}) according to the following two equations:

$$r_{ij} = [(x_j-x_i)^2 + (y_j-y_i)^2 + (z_j-z_i)^2]^{1/2}, \tag{3b}$$

$$\tau_{ij} = r_{ij}/c, \tag{3c}$$

where (x_i,y_i,z_i) are the spatial coordinates of the i th array element, (x_j,y_j,z_j) are the spatial coordinates of the j th field location, and c is the velocity of propagation of the media.

B. Definition of the mean-square error

The mean-square error (MSE) between an observed field and a desired field at some arbitrary set of spatial locations and for a specified set of discrete times is defined as follows:

$$\text{MSE} = \left(\frac{1}{TM}\right) \sum^{i} \sum^{j} [g_j(t) - y_j(t)]^2, \tag{4}$$

where $g_j(\ )$ is the desired field at the j th location, $y_j(\ )$ is the observed field at the j th location, t is the discrete time variable, and T is the total time interval. The goal is to find a

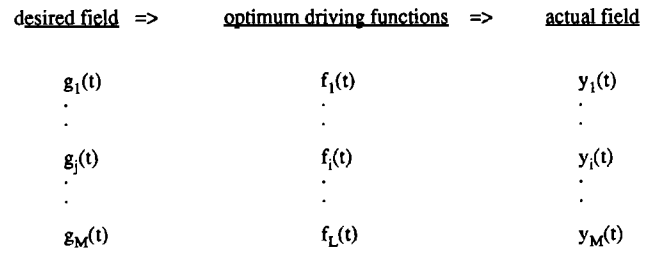

FIG. 2. Synthesis problem: Find a set of driving functions $f_i(t)$ that will produce a field $y_j(t)$ similar to the desired field $g_j(t)$.

set of optimum driving functions (f_i) that will minimize the MSE. This concept is illustrated in Fig. 2.

C. Derivation of the optimum driving functions (MSE sense)

We proceed by equating the functional derivative (partial with respect to the driving functions) of the expression for the MSE to zero.

Taking the functional derivative we obtain,

$$\frac{\partial \text{MSE}}{\partial f_k(\tau)} = -\left(\frac{1}{TM}\right)\sum^{i}\sum^{j} 2[g_j(t) - y_j(t)]\frac{\partial y_j(t)}{\partial f_k(\tau)}. \tag{5a}$$

From Eq. (3a), we observe that

$$\frac{\partial y_j(t)}{\partial f_k(\tau)} = \begin{cases} 1/(4\pi r_{kj}), & t = \tau + \tau_{kj} \\ 0, & \text{otherwise} \end{cases}. \tag{5b}$$

Substituting (5b) into (5a) and equating the result to zero, we obtain

$$0 = \sum^{j} \frac{[g_j(\tau + \tau_{kj}) - y_j(\tau + \tau_{kj})]}{r_{kj}}. \tag{6}$$

Substituting (3) into (6) then gives,

$$\sum^{j} \frac{g_j(\tau + \tau_{kj})}{r_{kj}} = \sum^{j}\sum^{i} \frac{f_i(\tau + \tau_{kj} - \tau_{ij})}{(4\pi r_{kj} r_{ij})}, \tag{7}$$

for $1 \leqslant i \leqslant L$, $1 \leqslant j \leqslant M$, $1 \leqslant k \leqslant L$.

D. Solving the set of linear equations

Equation (7) represents a set of linear equations which can be solved for the set of optimum driving functions $f_i(t)$. We first formulate Eq. (7) in matrix form and then solve the resulting matrix system for the driving functions. This can be easily accomplished by formulating Eq. (7) in the frequency domain.

Taking the Fourier transform of Eq. (7), we obtain

$$\sum^{j} \frac{p^{\tau_{kj}} G_j(\omega)}{r_{kj}} = \sum^{j}\sum^{i} \frac{p^{(\tau_{kj} - \tau_{ij})} F_i(\omega)}{(4\pi r_{kj} r_{ij})}, \tag{8}$$

where $p^{\tau_{kj}} = e^{(j\omega\tau_{kj})}$, $F_i(\omega)$ is the Fourier transform of $f_i(t)$, and $G_j(\omega)$ is the Fourier transform of $g_j(t)$.

We can now rewrite Eq. (8) as

$$\sum^{j} h^{*}_{kj} G_j(\omega) = \sum^{j} h^{*}_{kj} \sum^{i} h_{ij} F_i(\omega), \tag{9}$$

where $h_{ij} = p^{-\tau_{ij}}/(4\pi r_{ij})$, $h^{*}_{kj} = p^{\tau_{kj}}/(4\pi r_{kj})$. For a fixed frequency (ω), we have L equations which can be written in matrix form as follows:

$$\mathbf{H}^{\dagger}\mathbf{g} = \mathbf{H}^{\dagger}\mathbf{H}\mathbf{f}, \tag{10}$$

where

$$\mathbf{f} = \begin{vmatrix} F_1 \\ \vdots \\ F_L \end{vmatrix}, \quad \mathbf{g} = \begin{vmatrix} G_1 \\ \vdots \\ G_M \end{vmatrix} \quad \mathbf{H} = \begin{vmatrix} h_{11} & \cdots & h_{1L} \\ \vdots & \ddots & \vdots \\ h_{M1} & \cdots & h_{ML} \end{vmatrix},$$

$$\mathbf{H}^{\dagger} = \begin{vmatrix} h^{*}_{11} & \cdots & h^{*}_{1M} \\ \vdots & \ddots & \vdots \\ h^{*}_{L1} & \cdots & h^{*}_{LM} \end{vmatrix}.$$

Solving for $\mathbf{f}$, we obtain

$$\mathbf{f} = (\mathbf{H}^{\dagger}\mathbf{H})^{-1}\mathbf{H}^{\dagger}\mathbf{g}. \tag{11}$$

If $L = M$ and $\mathbf{H}$ is nonsingular, then Eq. (11) reduces to the matrix equation

$$\mathbf{f} = \mathbf{H}^{-1}\mathbf{g}. \tag{12}$$

In this case, we can always obtain an exact solution.

E. The propagation equation

We now present a more intuitive derivation of the least-squares solution to the inverse propagation problem presented in the previous sections. We note that Eq. (3a) has the frequency domain representation

$$\mathbf{g} = \mathbf{H}\mathbf{f}. \tag{13}$$

This result is readily obtained by following the same procedure presented in the previous section. We refer to this relationship as the *propagation equation*. Note that each element of the matrix $\mathbf{H}$ provides the necessary attenuation and phase correction factors to propagate the corresponding frequency component of each array element to the observation points. We refer to the matrix $\mathbf{H}$ as the *propagation matrix*. The least-squares solution to Eq. (13) is well known[2] and it is given by Eq. (11), where the expression $(\mathbf{H}^{\dagger}\mathbf{H})^{-1}$ is commonly referred to as the *pseudoinverse* of the matrix $\mathbf{H}$.

F. Summary

Based on a point source propagation model in a homogeneous media, we have derived a least-squares solution to the inverse propagation problem (given an arbitrary field, find the corresponding driving functions of a given array of radiating elements). This solution is obtained by solving a set of linear equations in the frequency domain for each frequency component. The right-hand side of the matrix equation is defined by the product of the propagation matrix and a field vector. The field vector consists of spatial samples of the field, while the propagation matrix is a function of the relative distances between the array elements and the set of spatial locations that define the field. In the next section, we apply this technique to the LW problem.

II. COMPUTER SIMULATIONS

This section illustrates the feasibility of the proposed technique for calculating the driving functions of an array required to generate localized waves. All the results were

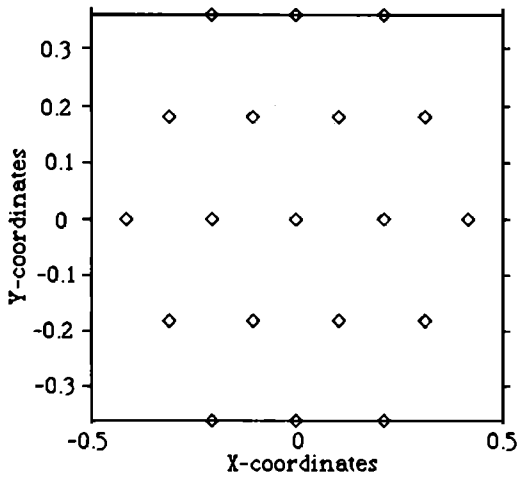

FIG. 3. Geometry of the source array (19 elements, 1-cm aperture).

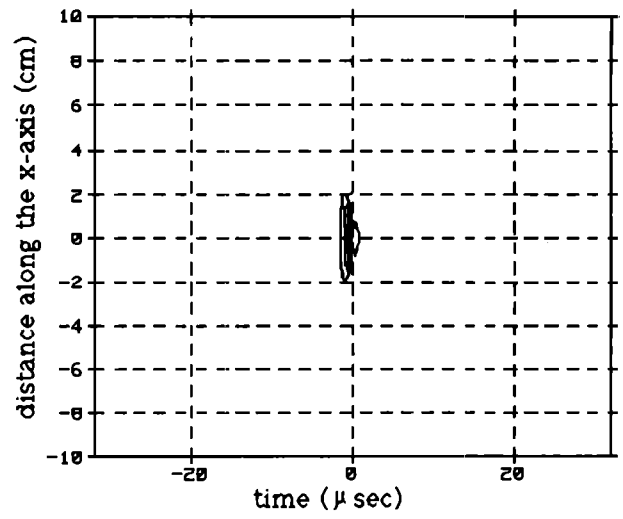

FIG. 4. MPS source-free solution after traveling a distance of 30 cm.

obtained by computer simulation based on the point source propagation model formulated in Sec. I. The computer simulations were done on a SUN-3 workstation using single precision arithmetic. The signal processing package SIG (General Purpose Signal Processing Program)[3] was used as the development environment for implementing all the numerical calculations as well as for plotting the results. A conjugate gradient algorithm[4–6] is used to solve the propagation equation in all cases.

The two cases are investigated. In the first case, a LW source-free solution to the wave equation is used as the desired field. This case is intended to illustrate the feasibility of the least-squares approach for generating array driving functions to generate source-free solutions to the wave equation, specifically for producing localized wave energy. In the second case, a numerical traveling impulse is defined as the desired field. We compare the resulting fields for both cases, the LW source-free solution and the traveling impulse, with the field generated by driving the array uniformly with a cw signal. The performance of each set of results is quantified in terms of the beam spreading and the energy efficiency as a function of the distance traveled from the array.

The array that has been selected for the following examples consists of a 1-cm aperture array with a total of 19 array elements. All the array elements lie on the X-Y plane and they have been arranged as depicted in Fig. 3.

A. LW source-free solution example

The LW source-free solution selected for our simulations is the acoustic modified power spectrum (MPS) pulse:[1,7,8]

$$f(x,y,z,t) = \frac{1}{z_0 + j(z-ct)} \frac{1}{(s/\beta + a)^{\alpha}} e^{-bs/\beta}, \quad (14)$$

where $z_0 = 4.5 \times 10^{-2}$ cm, $b = 6.0\,\text{cm}^{-1}$, $\beta = 300$, $a = 100$ cm, $\alpha = 1.0$, and

$$s(x,y,z,t) = \frac{x^2 + y^2}{z_0 + j(z-ct)} - j(z+ct).$$

The propagation media is assumed to be water with a velocity of propagation (c) of 1.5×10^5 cm/s. It is assumed that

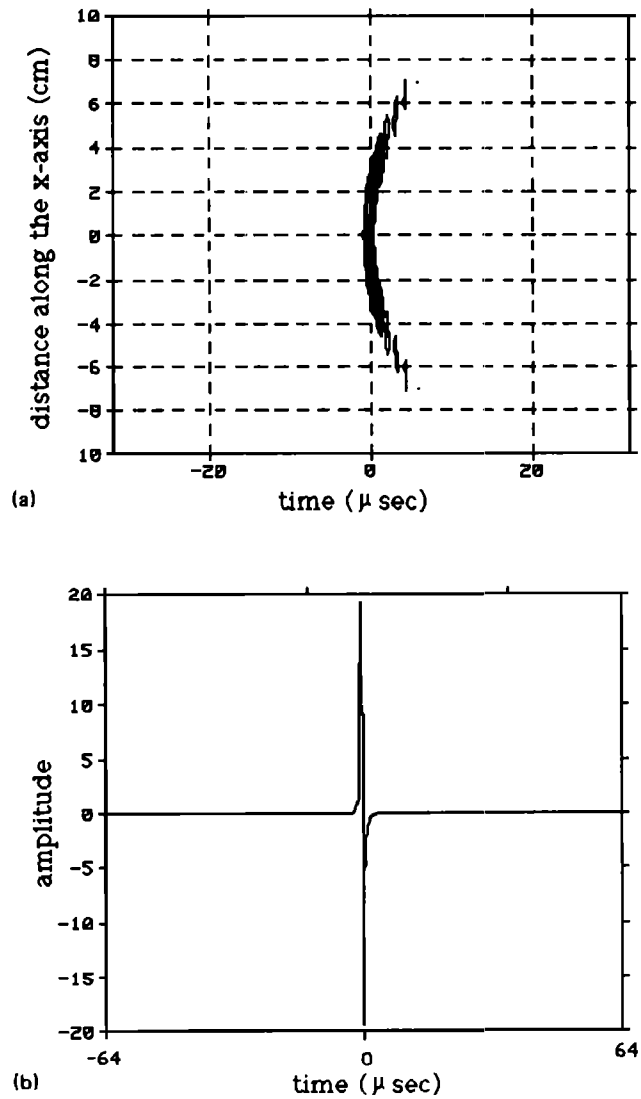

FIG. 5. (a) Reconstructed MPS field based on Huygen's principle, (b) driving function for the center element of the array.

the pulse is propagating along the Z axis. Figure 4 shows contour levels of the energy distribution of the MPS field as a function of time, and distance along the X (or Y) axis after traveling a distance of 30 cm (since this particular LW solution is circularly symmetric, it is sufficient to specify the field along the X or Y axis). The reference time $t = 0$ represents the time at which the center of the pulse arrives at $z = 30$ cm.

A simple procedure for reconstructing this field using an array of point sources is to excite the array elements with a set of driving functions derived from the original source-free solution using Huygen's principle.[9] Figure 5 shows the field generated by driving the array depicted in Fig. 3 with those signals. One of the array driving functions is also shown.

Before comparing this field with the one obtained with the least-squares approach, we must discuss the strategy used to sample the field of the MPS source-free solution.

B. Sampling the desired field

In order to apply the least-squares approach, we must sample the desired field at a finite number of locations and time intervals. Our strategy is to sample the field based on sampling theory concepts. Let us first consider the temporal and spatial characteristics of the MPS source-free solution. Figure 6 shows a surface and contour plot of the magnitude in dB's of the MPS field at $z = 30$ cm. Note that the pulse has been defined so that its peak amplitude occurs at $x = y = 0$ and at $t = 0$. The figure shows that it takes a time span of 128 μs and an aperture size of 250 cm for the pulse amplitude to decrease approximately 45 dB (a factor of about 200) with respect to its peak value.

Figure 7 illustrates the spectral characteristics of the MPS source-free solution. Note that near the origin, the pulse is wideband in nature, having a bandwidth of approximately 2 MHz (-45-dB point). In order to preserve this bandwidth, the field must be sampled at a rate of about 4×10^6 samples/s (twice the highest frequency) in order to avoid *aliasing* effects.

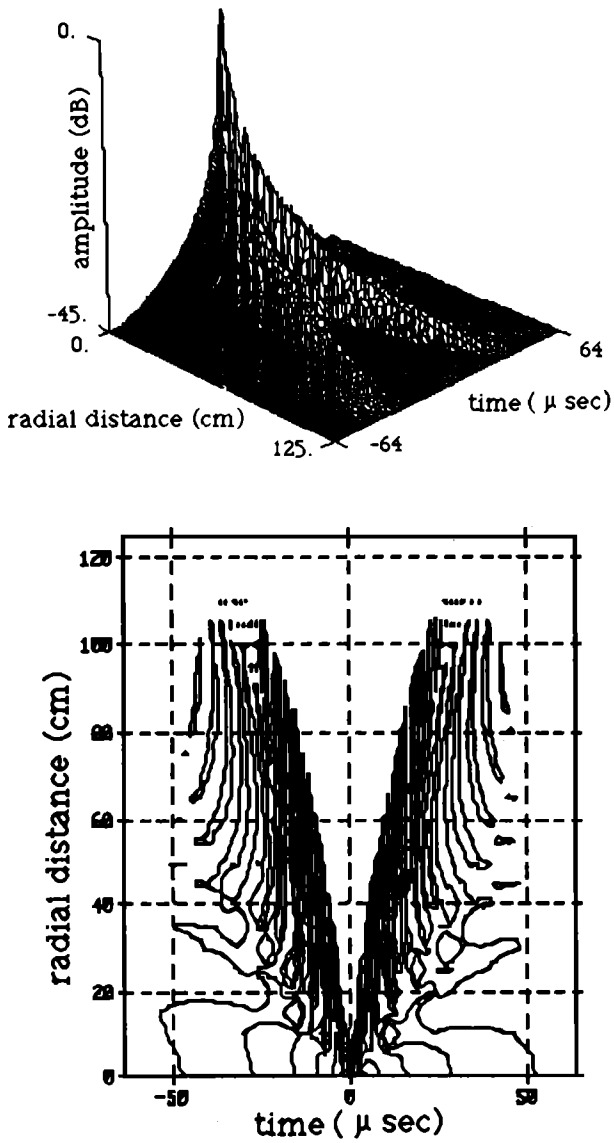

FIG. 6. Temporal and spatial characteristics of the MPS field at $z = 30$ cm.

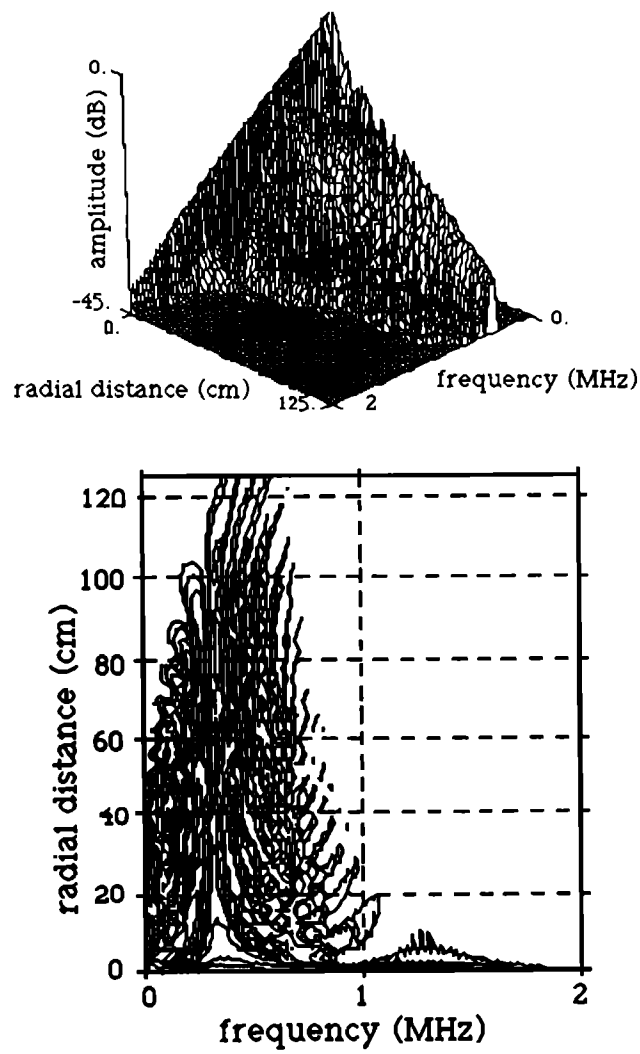

FIG. 7. Spectral characteristics of the MPS field at $z = 30$ cm.

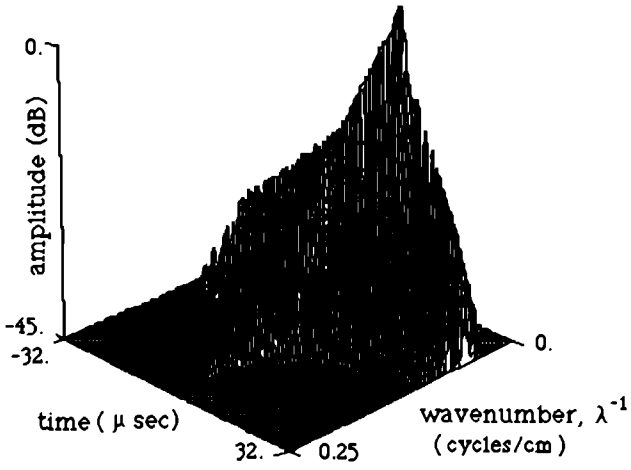

FIG. 8. Wave number spectrum of the MPS field at $z = 30$ cm.

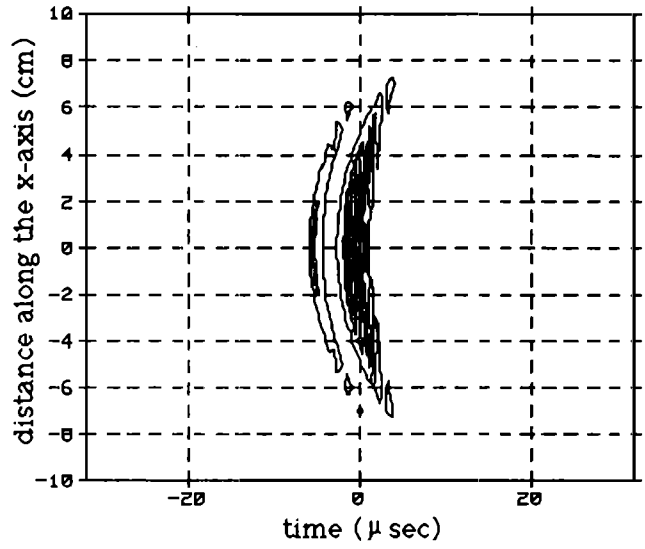

FIG. 9. Reconstructed MPS field based on the least-squares approach.

The wave-number spectrum of the MPS field is shown in Fig. 8 as a function of time. Note that the shortest spatial wavelengths are on the order of 4 cm long (− 45-dB point). Based on the shortest wavelength of the field, we can calculate the minimum *sampling density* (number of samples per unit area) required to minimize spatial aliasing effects. If we use a *hexagonal sampling* scheme[10] (which provides an efficient method of sampling circular symmetric, bandlimited spatial signals), then the sampling density is given by $2\sqrt{3}/\lambda^2_{\min}$, where $\lambda_{\min}$ stands for the shortest wavelength to be sampled. Therefore, for a 4-cm wavelength, the sampling density should be on the order of 0.2 samples/cm^2. Observe that a hexagonal sampling scheme was also used to arrange the array elements of the source array (see Fig. 3).

Table I summarizes the requirements for selecting the temporal and spatial samples of the MPS field (based on sampling theory concepts) to be used for calculating the driving functions of the source array using the least-squares approach. Based on these results we need a total of 512 temporal samples (or 256 frequency components, neglecting the dc term) at 9800 different spatial locations. In terms of the number of mathematical computations involved, this problem requires the solution of 256 linear systems of complex equations of order 19×9800. Unfortunately, the number of spatial locations is directly proportional to the squared value of the aperture size, and it is also proportional to the squared value of the spatial bandwidth $(1/\lambda_{\min})^2$. Therefore, in order to reduce the number of spatial locations (and, therefore, the number of computations), we have to either reduce the sampling density or reduce the aperture size. (Another option would be to use a different sampling strategy which will not be considered at this time). Since the short wavelengths are important in order to preserve the localized behavior of the solution (which is the main feature that we are trying to duplicate), it is more desirable to reduce the size of the receiving aperture.

TABLE I. Sampling requirements of the MPS field at $z = 30$ cm.

Sampling rate	4×10^6 samples/s
Sampling density	0.2 samples/cm^2
Time span	128 μs
Aperture size	250 cm

C. Least-squares solution to the LW source-free example

We now compare the field generated with the Huygen's approach with the field generated from the same array using a set of driving functions obtained with the proposed least-squares approach. The resulting field is shown in Fig. 9. Note that although the beam is not as localized as the exact field (Fig. 4), spatially, it is very similar to the beam generated from the Huygens reconstruction approach (Fig. 5).

This reconstructed MPS field was generated using the sampling parameters from Table I with a receiving aperture size of 40 cm instead of 250 cm. This reduced the number of spatial locations needed for sampling the field from 9800 to 250.

Based on other computer simulations not shown here, our studies indicate that increasing the value of the sampling parameters (sampling rate, sampling density, and time span) tend to generate smoother energy profiles than the one shown in Fig. 9, but the localized characteristics of the resulting field remain about the same.

D. The array driving functions

Our studies show that the least-squares solution to the inverse propagation problem tends to generate very large low-frequency components which do not seem to be necessary in order to generate a localized field. Although, at this point, this behavior is not well understood, we suspect that due to the particular geometry of our problem (array elements as well as selected field locations are very close together in comparison to the traveled distance), the inverse problem is "ill-conditioned" at the low frequencies. We have investigated two ways of suppressing these strong, low-frequency resonances in the driving functions. For the first ap-

proach we high-pass filter the calculated driving functions in order to attenuate the low-frequency resonances. It also helps to taper the ends of the resulting time series after the filtering operation. This can be easily accomplished by multiplying the driving functions times a Hanning (or similar) window function. In the second approach we apply an energy constraint to the inverse problem (see last section of the Appendix). This approach tends to keep the number of resonances to a minimum.

Figure 10 shows the solution to the MPS example in both, the time and frequency domains, for the center element of the array. The first pair of plots shows the original solution to the MPS source-free inverse problem. Note the strong resonance at the low frequencies which is responsible for the

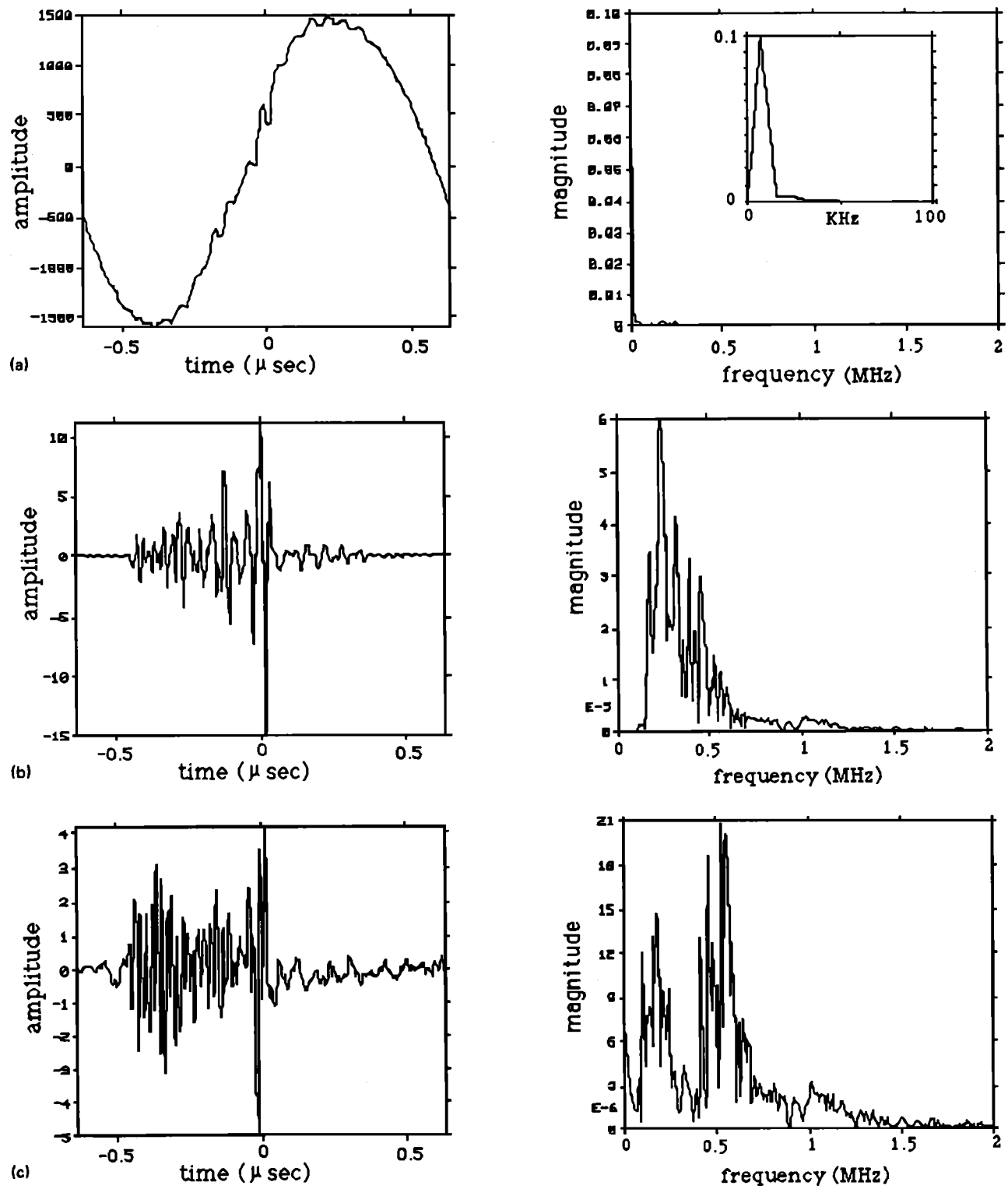

FIG. 10. Least-squares solutions in the time and frequency domains to the MPS source-free problem for the center element of the array: (a) unconstrained solution, (b) filtered solution, (c) solution with an energy constraint.

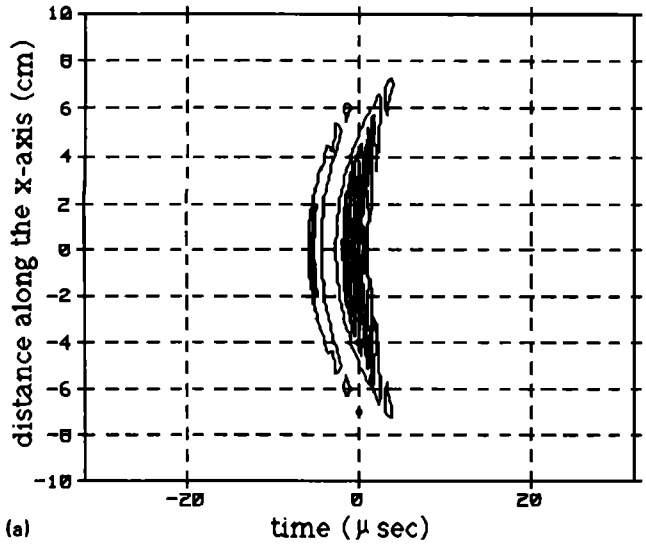

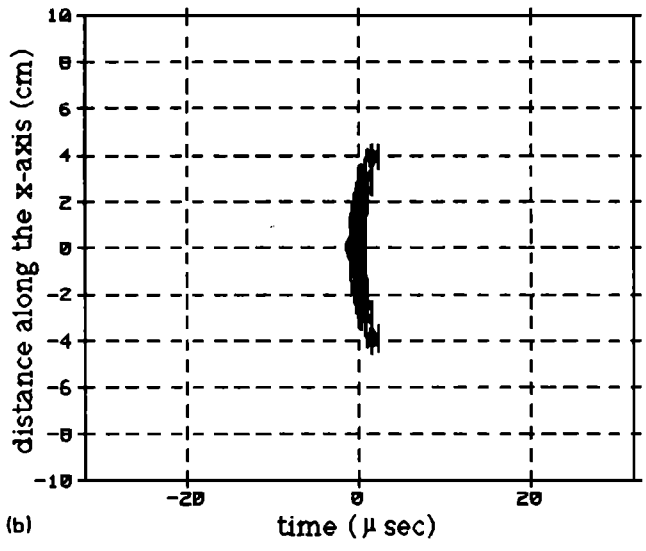

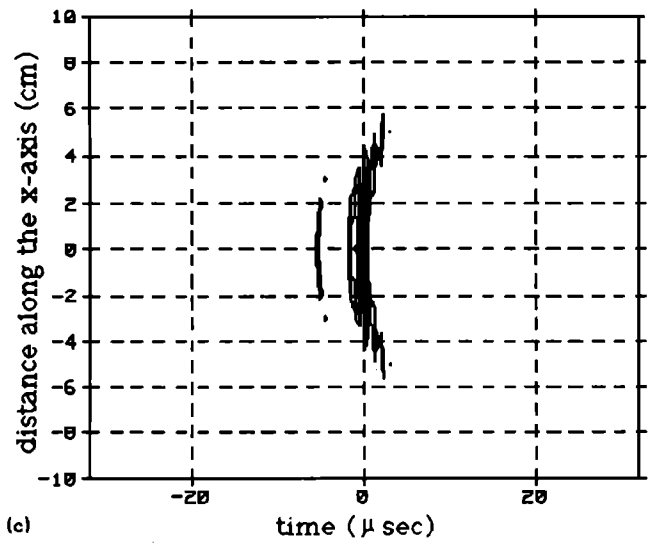

FIG. 11. Comparison of the reconstructed energy field from the (a) unconstrained solution, (b) filtered solution, (c) solution with an energy constraint.

very large amplitudes and the sinusoidal waveshape of the driving function. The next pair of plots illustrates the high-pass filtering approach. In this case, the resonances have been suppressed considerably, thus reducing the amplitude levels of the driving functions considerably. The waveform has also been tapered at the ends by using a Hanning window. The last pair of plots shows the solution to the same problem applying an energy constraint to the inverse problem, i.e., the sum of the squares of the driving functions is constrained to be a constant as well. This energy constraint was implemented using the conjugate gradient algorithm discussed in the Appendix. Although there are still some resonances present in the frequency spectrum, they are much smaller than the resonances of the unconstrained solution. Note the ringing in the early-time portion of the driving functions, which is caused by the remaining resonances present in the solution.

The corresponding fields at $z = 30$ cm are depicted in Fig. 11 for the above three cases. Note that the results for the

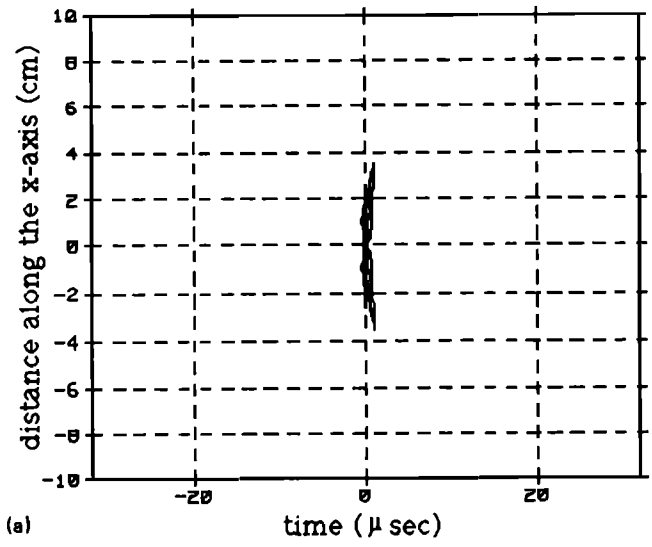

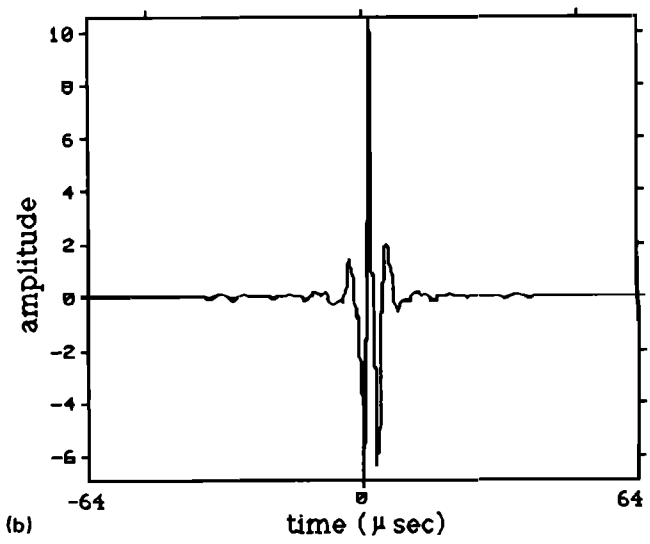

FIG. 12. Traveling impulse least-squares solution: (a) reconstructed field, (b) driving function for the center array element.

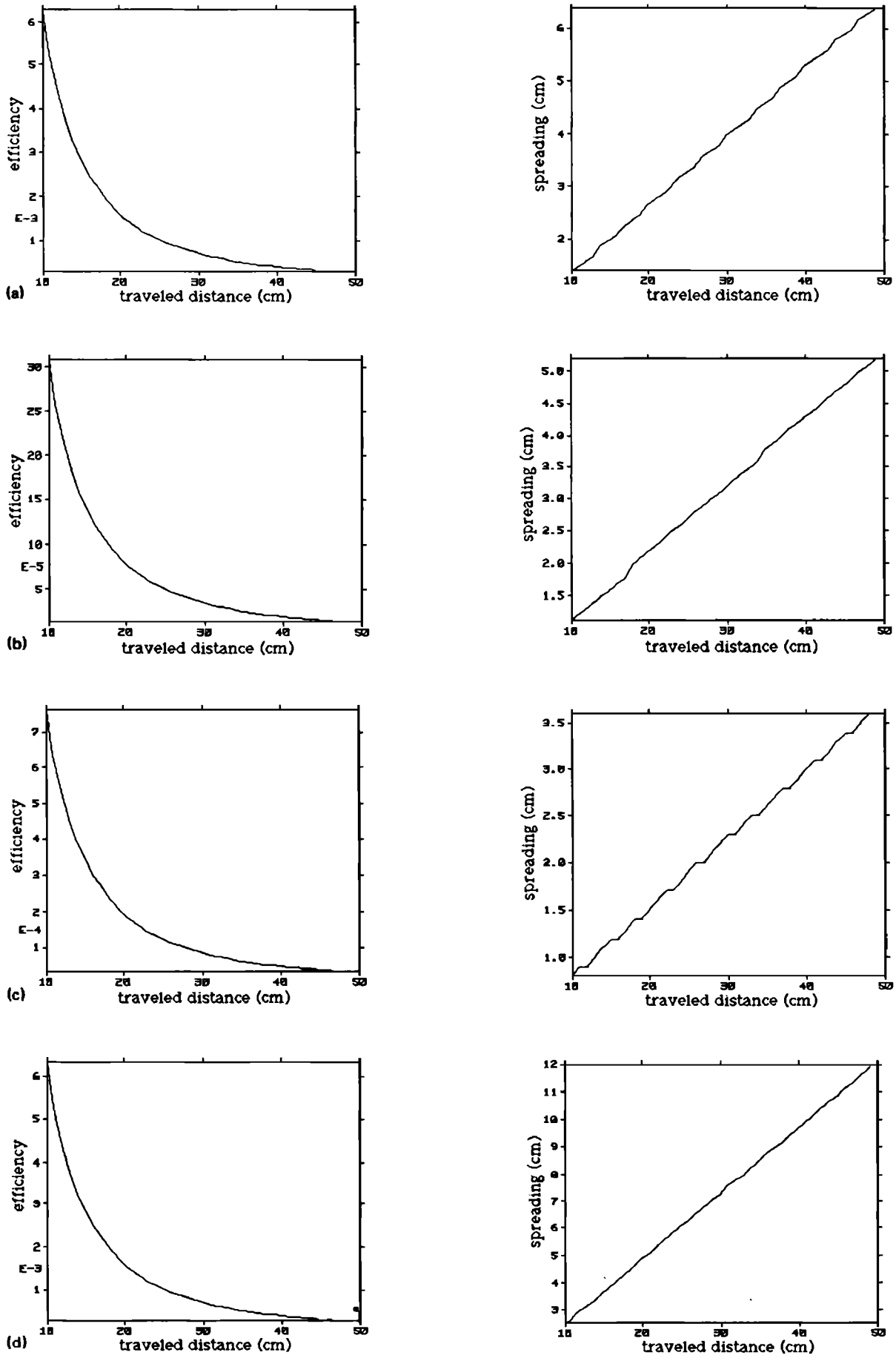

FIG. 13. Comparison of the beam performance (efficiency and spreading) for the following cases: (a) MPS using Huygens approach, (b) MPS using least squares with filtering, (c) traveling impulse using least squares with filtering, (d) cw at 345 kHz.

constrained and the filtered cases are very similar. Moreover, both cases produce a beam more localized than the beam generated from the Huygens reconstruction approach (Fig. 5).

E. Traveling impulse example

Ideally, the ultimate wave pulse for the transmission of localized wave energy is a traveling impulse function. Although such a pulse cannot be realized physically, a least-squares solution to the traveling impulse problem can be obtained by defining the desired field to be the (numerical) unit impulse function, i.e., a field with a value of one at $x = y = 0$ and $t = z/c$, and a value of zero everywhere else. Figure 12 shows the solution to this problem using the same sampling parameters that were used for the MPS field example. Note that the solution to the traveling impulse problem gives a more localized field than the one obtained for the MPS source-free problem, given the same source array and the same sampling parameters.

F. Performance study

We now compare the performance of the different solutions against each other and against the classical cw beam. This comparison is accomplished by calculating the efficiency of the beam and its spreading as a function of the distance the transmitted beam has propagated from the array for each set of driving functions. The efficiency of the beam is defined as the ratio of the on-axis beam energy to the total energy of the integral of the array driving functions as a function of the distance traveled by the beam. This quantity is given by the following formula:

$$\text{efficiency } (z_0) = \frac{4}{c^2} \frac{\int |y(z_0,t)|^2 \, dt}{\Sigma \int |\int^t f_i(t) dt|^2 \, dt}, \tag{15}$$

where $y(\ )$ represents the field on-axis ($x = y = 0$) at $z = z_0$. The factor $(4/c^2)$ has been introduced to make our results conform to the far field expression obtained from Huygens' representation, i.e., $(2/c)y(\ )\Sigma^{i\partial_t g_i(\ )}/2\pi cr$, where $g(\ )$ is the signal delivered to the i th element of the array. Our driving functions are the signals leaving the array, i.e., $f_i(\ ) = (\partial/\partial t)\, g_i(\ )$. Moreover, in order to simplify the implementation of the software, we expressed all distances in units of the speed of propagation, in this case centimeters. The term $\int^t f_i(\ )dt$ is the integral of the i th driving function of the array. It represents the signal $g_i(\ )$ delivered from a power source to the i th element of the array.

The beam spreading is defined as the radial distance from the z axis (the center of the beam) to the point at which the beam energy decays to half its on-axis value. This quantity is also a function of the traveled distance of the beam. The energy spreading and efficiency results for all the cases previously discussed are shown in Fig. 13. All the results corresponding to the least-squares approach were high pass filtered as previously discussed. The first set of curves corresponds to the field generated by using the MPS source-free solution via the Huygens' approach. The second set corresponds to the least-squares solution to the MPS source-free case. The third set corresponds to the least-squares solution to the traveling impulse case. The fourth case was generated by exciting each array element with a 345-kHz cw signal. This frequency corresponds to the effective frequency of the driving functions delivered to the array that were generated via Huygens approach. The effective frequency (f_{eff}) represents a measure of the "maximum" frequency of the signals driving the array, and it is defined by the expression:

$$(2\pi f_{\text{eff}})^2 = \frac{\Sigma \int |f_i(t)|^2 \, dt}{\Sigma \int |\int^t f_i(t) dt|^2 \, dt} = \frac{\Sigma \int |\partial_t g_i(t)|^2 \, dt}{\Sigma \int |g_i(t) dt|^2 \, dt}. \tag{16}$$

All the results including the effective frequency of the driving functions for all cases are summarized in Table II. The results based on the least-squares approach were generated with filtering, and with an energy constraint plus filtering. We have also included the results for the 2-MHz cw case. This frequency corresponds to the maximum allowed bandwidth in all of the cases. Note that excluding the 2-MHz case, the traveling impulse solution produces the most localized beam. Furthermore, the least-squares solution to the MPS example shows an improvement in energy spreading over the Huygens approach of calculating the array driving functions. Note that the beams corresponding to the least-squares approach are not very efficient. We believe this is due to the fact that in spite of the energy constraint imposed on the solution and the high-pass filtering, there are still some resonances present in the driving functions due to the geometry of our problem. The fields associated with these low-frequency resonances expand rapidly, hence, the amplitudes decrease quickly once they leave the array. However, they require a significant amount of energy to generate them. Thus these fields increase only slightly the spreading characteristics of the propagated beam, but decrease significantly the overall efficiency of the array.

Note that we used a cw signal of infinite time duration. This signal was the easiest to implement with the Fourier approach. Cases were tested in which finite record length cw signals or tone bursts were used to drive the array. The fields

TABLE II. Summary of the beam performance at $z = 50$ cm for: (1) the lw example via Huygens approach, (2) least squares with filtering, (3) least squares with an energy constraint and filtering, (4) the traveling impulse example using least squares with filtering, (5) least squares with an energy constraint and filtering, (6) cw at 345 kHz, (7) cw at 2 MHz.

Case	Effective freq.	Efficiency	Spreading (cm)
Huygens	345 kHz	$2.6\times10-4$	6.4
lw-least square w/HPF	258 kHz	$1.3\times10-5$	5.2
w/constraint + HPF	476 kHz	$1.3\times10-4$	5.6
impls-least square w/HPF	249 kHz	$3.2\times10-5$	3.6
w/constraint + HPF	836 kHz	$1.3\times10-3$	3.6
cw @ effective freq.	345 kHz	$2.6\times10-4$	11.9
cw @ maximum freq.	2 MHz	$8.9\times10-3$	2.1

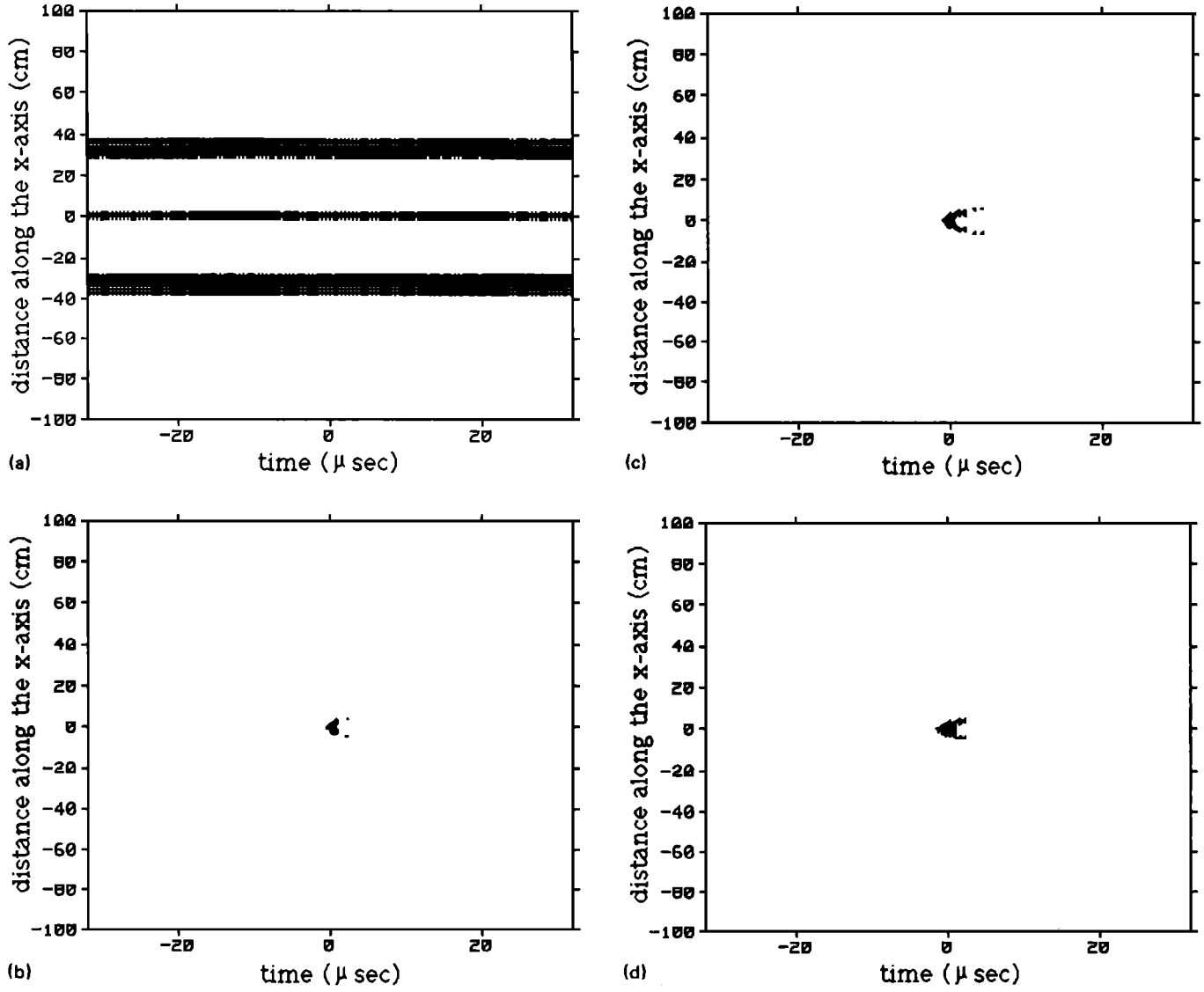

FIG. 14. Field at $z = 30$ cm corresponding to: (a) cw @ 2 MHz, (b) least-squares approximation to an ideal traveling impulse, (c) MPS via Huygens, (d) MPS via least squares with filtering.

generated with the tone burst driving functions were typically 40% less efficient than the pure cw case. The decrease in efficiency results from an increase in the leakage to the field outside the main beam. Since the infinite time record cw case is not achievable in practice, the cw performance noted here is better than one could realize physically, making the comparisons presented here the most stringent that one could achieve.

In summary, the proposed least-squares approach is suitable for calculating array driving functions for generating lw source-free solutions to the wave equation. In all cases, the least-squares solution produces a beam with better spreading characteristics than its cw counterpart (cw signals with the same effective frequency). Furthermore, solving the traveling impulse problem seems to generate a beam whose mainlobe characteristics are almost as good as the 2-MHz cw case. Although the 2-MHz cw case shows a more localized beam with higher efficiency when compared to all the other results, this case suffers from much larger sidelobe levels than any of the other cases as illustrated in Fig. 14. These sidelobe levels appear because the wavelength of the 2-MHz signal is much smaller than the separation distance between the source array elements.

III. SUMMARY AND CONCLUSIONS

This paper presents a framework for calculating an optimum (least-squares sense) set of driving functions for an array of point sources given a scalar representation of the desired field. The problem is formulated as a set of linear equations in the frequency domain. We have demonstrated the use of the proposed framework for calculating array driving functions to generate localized wave energy. Two cases are considered: (1) a lw source-free solution to the wave equation, and (2) a numerical traveling unit impulse. Both cases show an improvement in energy spreading and in energy efficiency when compared to the cw case for the corresponding effective frequency of the driving functions. Fur-

thermore, there are no sidelobes effects. The least-squares approach appears to be suitable for generating localized-wave source-free solutions to the wave equation. Moreover, based on the different cases that were studied, defining the desired field to be a traveling impulse function gives the most localized and efficient beam for a given bandwidth excluding the cw case which suffers from sidelobes.

Our studies show that the proposed technique tends to generate very large low-frequency components which do not seem to be necessary in order to generate a localized field. We suspect that due to the particular geometry of the localized energy problem (array elements as well as selected field locations are very close together in comparison to the traveled distances), the inverse problem is "ill-conditioned" at the very lowest frequencies. These large resonances can be reduced by high pass filtering the driving functions. They can also be minimized by solving the inverse problem with an energy constraint on the solution. This approach and several other possible alternate approaches are discussed in the Appendix to follow.

ACKNOWLEDGMENTS

The authors would like to acknowledge the contribution of this work of Dennis Goodman and Frederick Followill. We would also like to acknowledge Robert Sherwood and John Dias for their software and computer support. Work was performed under the auspices of the U.S. Department of Energy by the Lawrence Livermore National Laboratory under Contract W-7405-Eng-48.

APPENDIX

In this Appendix, we discuss some modified versions of the least-squares solution to the inverse propagation problem. Although we have not implemented these approaches (with the exception of the conjugate gradient method), they are alternatives to the one presented, and are currently being investigated.

1. The weighted MSE solution to the propagation equation

Let us consider the case where a large number of field locations are specified relative to the number of array elements ($M \gg L$). Since in this case there is no guarantee that there exists a set of driving functions that can reproduce the desired field at all the specified locations, we consider weighting the error function. This is useful in cases where a degradation in performance at some locations is acceptable at the expense of improving the performance at some other locations.

We start by redefining the cost function to be minimized as,

$$\mathrm{WMSE} = \sum^{i} \sum^{j} w_j [g_j(t) - y_j(t)]^2, \tag{A1}$$

where w_j is the weighting factor for the error at the jth location.

Minimizing the new cost function gives rise to a set of linear equations similar to the ones formulated previously in Sec. I [see Eqs. (5a)–(7)],

$$\sum^{j} \frac{w_j g_j(\tau + \tau_{kj})}{r_{kj}} = \sum^{j} \sum^{i} \frac{w_j f_i(\tau + \tau_{kj} - \tau_{ij})}{(4\pi r_{kj} r_{ij})}. \tag{A2}$$

We proceed again by formulating the problem in the frequency domain in order to solve for the driving functions. After taking the Fourier transform and simplifying the notation as we did previously [see Eqs. (8) and (9)], we obtain

$$\sum^{j} w_j h^*_{kj} G_j(\omega) = \sum^{j} w_j h^*_{kj} \sum^{i} h_{ij} F_i(\omega). \tag{A3}$$

We can now rewrite Eq. (A3) in matrix form as,

$$\mathbf{W}^\dagger \mathbf{g} = \mathbf{W}^\dagger \mathbf{H} \mathbf{f}, \tag{A4}$$

where

$$\mathbf{W}^\dagger = \begin{vmatrix} w_1 h^*_{11} & \cdots & w_M h^*_{1M} \\ \vdots & \ddots & \vdots \\ w_1 h^*_{L1} & \cdots & w_M h^*_{LM} \end{vmatrix}.$$

We refer to W as the *weighted propagation matrix*. Notice that if $L = M$ and H is nonsingular, Eq. (A4) reduces back to Eq. (12), which is independent of the weighting factors w_j. This is expected since in this particular case there exists an exact solution to the inverse problem, and therefore, minimizing the MSE is the same as minimizing the weighted MSE (WMSE).

2. Energy constrained solution to the propagation equation

It is of interest in some applications to find solutions to the propagation equation that constrain the total energy of the driving functions. From a mathematical point of view, we want to solve a set of linear equations (the propagation equation) such that the squared norm of the solution vector does not exceed some maximum value ξ, i.e.,

$$\text{solve } \mathbf{g} = \mathbf{H}\mathbf{f}, \quad \text{subject to } \|\mathbf{f}\|_2 \leqslant \xi. \tag{A5}$$

The solution to this minimization problem is given by

$$\mathbf{f} = [\mathbf{H}^\dagger \mathbf{H} + \kappa \mathbf{I}]^{-1} \mathbf{H}^\dagger \mathbf{g}, \tag{A6}$$

where κ is a decreasing function of ξ and is called the *biasing parameter.*[7]

3. A modified steepest descent approach

We now consider an iterative method for computing the driving functions based on a steepest descent approach. The basic idea is to iteratively cause incremental changes on the driving functions based on the gradient of the MSE. This procedure can be formulated mathematically as

$$f_k(\tau)^{\mathrm{new}} = f_k(\tau)^{\mathrm{old}} - \frac{\mu}{2} \frac{\partial \mathrm{MSE}}{\partial f_k(\tau)}. \tag{A7}$$

The parameter μ is a constant that governs the stability and the rate of convergence of the algorithm.[11]

After combining Eqs. (5a) and (5b), we can rewrite Eq. (A7) as

$$f_k(\tau)^{\mathrm{new}} = f_k \tau)^{\mathrm{old}} + (TM)^{-1} \mu \sum^{j} \frac{e_j(\tau + \tau_{kj})}{(4\pi r_{kj})}. \tag{A8}$$

If instead we wanted to minimize the WMSE, then (A7) becomes,

$$f_k(\tau)^{\text{new}} = f_k(\tau)^{\text{old}} + (TM)^{-1}\mu \sum^{j} \frac{w_j e_j(\tau + \tau_{kj})}{(4\pi r_{kj})}. \tag{A9}$$

One disadvantage of the current form of Eq. (A8) or (A9) is that unless the parameter μ is allowed to vary, the adjustments made to the driving functions from each available location will depend on the traveled distance r_{kj}. Field samples from far away locations will contribute a smaller adjustment than relatively closer field samples. This is due to the explicit $(1/r_{kj})$ factor in Eq. (A8) as well as the implicit $(1/r_{kj})$ factor in the error function itself. This dependency can be removed by scaling the error function by the square of the corresponding traveled distance. This allows all the field samples to contribute equally to the adjustment of the driving functions while keeping the parameter μ constant. We can also compensate for the factor T^{-1} in order to make the choice of μ independent of the time duration of the functions. Therefore, a modified steepest descent solution is given by the expression,

$$f_k(\tau)^{\text{new}} = f_k(\tau)^{\text{old}} + M^{-1}\mu \sum^{j} 4\pi r_{kj} e_j(\tau + \tau_{kj}). \tag{A10}$$

Note that the steepest descent approach does not involve the inversion of matrices or the computation of Fourier transforms. However, it does require the propagation of the driving functions at the end of each iteration cycle in order to compute the error functions (e_j). This procedure, when implemented as formulated in Eq. (13), does require taking Fourier transforms as well as a vector-matrix multiplication for each frequency. However, it is possible to implement Eq. (A10) in the frequency domain and therefore, avoid taking Fourier transforms at each iteration cycle. Taking the Fourier transform of Eq. (A10) gives,

$$F_k(\omega)^{\text{new}} = F_k(\omega)^{\text{old}} + \mu \sum^{j} q_{kj} E_j(\omega), \tag{A11}$$

where

$$q_{kj} = M^{-1} 4\pi r_{kj} p^{\tau_{kj}}.$$

The equivalent matrix relation is given by

$$f^{\text{new}} = f^{\text{old}} + \mu \mathbf{Q} \mathbf{e}, \tag{A12}$$

where

$$\mathbf{Q} = \begin{vmatrix} q_{11} & \cdots & q_{1M} \\ \vdots & \ddots & \vdots \\ q_{L1} & \cdots & q_{LM} \end{vmatrix}.$$

We refer to $\mathbf{Q}$ as the *back propagation matrix* since basically it propagates the error functions back to the source locations.

The main motivation for using an iterative approach such as the one just described, is to solve problems where we have a very large number of field locations which might cover a wide range of distances. This situation can cause severe numerical problems when trying to invert the pseudoinverse of the propagation matrix $(\mathbf{H}^{\dagger}\mathbf{H})^{-1}$. The basic strategy is to break the total set of field locations into smaller sets and then apply the steepest descent approach, iterating over each subset of field locations. Since the iterative approach allows for an initial set of driving functions, we could first compute an optimum set of driving functions [see Eq. (11)] based on one of the subsets of field locations (perhaps the most important one), and then switch to the iterative approach.

4. Conjugate gradient method[6]

The propagation equation can be solved using a conjugate gradient method. This method is similar to a steepest descent approach. Although it is slightly more complicated to implement, it converges faster than the steepest descent method. As with the steepest descent method, the current gradient vector is computed at each iteration. However, a linear combination of previous direction vectors is also added to obtain a new conjugate direction vector along which the solution moves. This is the technique with which we had the most success. One nice feature of the conjugate gradient method is that it is very easy to implement the energy constrained solution (the sum of the squares of the solution is constrained to be a constant). This is done by controlling the number of iterations of the algorithm based on some criteria. The criteria used for generating the results in Sec. II is based on the apparent condition number of the propagation matrix. The particular code that was used allows the user to specify an upper limit for the condition number of the matrix. If this limit is exceeded, the code terminates the iteration procedure. We modified the code so that not only will it stop iterating,but it will also return the previous estimate of the solution. This seems to help since the solution can grow a lot in just one iteration, especially when the matrix is badly "ill-conditioned." For more information on the conjugate gradient technique, consult Refs. 4 and 5.

[1] R. W. Ziolkowski, "Localized transmission of electromagnetic energy," Phys. Rev. A **39**(4), 2005–2033(1989).

[2] A. Albert, *Regression and the Moore–Penrose Pseudo Inverse* (Academic, New York, 1972).

[3] D. Lager and S. Azevedo, SIG, A general purpose signal processing program, UCID-19912, University of California (1985).

[4] C. C. Page and M. A. Saunders, "LSQR: An algorithm for sparse linear equations and sparse least squares," ACM Trans. Math. Software **8**, 1 (March 1982).

[5] C. L. Lawson, R. J. Hanson, D. R. Kincaid, and F. T. Krogh, "Basic linear algebra subprograms for FORTRAN usage," ACM Trans. Math. Software **5**, 3 (September 1979), pp. 308–323 and 324–325.

[6] D. Goodman, private communications, LLNL, Livermore, California.

[7] R. W. Ziolkowski, D. K. Lewis, and B. D. Cook, "Evidence of localized wave transmission," Phys. Rev. Lett. **62**(2), 147–150 (1989).

[8] R. W. Ziolkowski, "Localized transmission of wave energy," Energy and Technology Review, Lawrence Livermore National Laboratory, UCRL-52000-88-11 (1988), p. 16–23.

[9] D. S. Jones, *The Theory of Electromagnetism* (Pergamon, New York, 1964).

[10] D. E. Dudgeon and R. M. Mersereau, *Multi-Dimensional Digital Signal Processing* (Prentice-Hall, Englewood Cliffs, NJ, 1984).

[11] B. Widrow and S. D. Stearns, *Adaptive Signal Processing* (Prentice-Hall, Englewood Cliffs, NJ, 1985).